Jurnal Ilmu Fisika
Vol. 17, No. 2, September 2025, pp. 171–181
ISSN: 1979-4657 (Print); 2614-7386 (Online)
https://doi.org/ 10.25077/jif.17.2.171-181.2025

Jurnal Ilmu Fisika
Open Access

Evaluation of Shear Wave Velocity Using Microtremor Data at Rammang-Rammang Maros Karst Area TN Babul

Sitti Hasaniyah[1], Muhammad Arsyad[2], Agus Susanto[2]

[1] Graduate Program of Universitas Negeri Makassar, Jl. Bonto Langkasa, Makassar, 90222, Indonesia
[2]Department of Physics, Universitas Negeri Makassar, Makassar, 90221, Indonesia

Article Info

Article History:

Received January 16, 2025
Revised May 14, 2025
Accepted May 29, 2025
Published online June 22, 2025

Keywords:

Rammang-Rammang
microtremor
HVSR curve
HVSR inversion
shear wave velocity

Corresponding Author:

Sitti Hasaniyah,
Email:
sittihasaniyah14@gmail.com

ABSTRACT

This study aims to identify the profile of shear wave velocity *(Vs_{30})* and to analyze the classification of soil types of the Rammang-Rammang Maros Karst Area based on Vs_{30} value. This research was carried out at Rammang-Rammang Maros Karst Area, Salenrang and Bontolempangan Village, Bontoa District, Maros Regency, South Sulawesi. The method used in this research was the Horizontal to Vertical Spectral Ratio (HVSR) method to produce the HVSR curve and then analysed in the inversion method using Dinver to produce a ground profile. The Vs_{30} values were obtained in the range from 249 to 1384 m/s. The characteristics of the rock response could indicate the specifications of a rock type. Based on the Vs_{30} values, it was found that the classification of rock *(S_B)* located around the karst hilly areas, soft rock *(S_C)* located around the residential areas and the river, and stiff soil *(S_D)* located near ricefield. The overall seismic risk in the research area is low based on Vs_{30} values below 200 m/s. These findings provide essential baseline data to support sustainable land use and tourism development planning in the region.

1. INTRODUCTION

Karst is a landscape formed in soluble rocks, mainly carbonate rocks due to karstification processes that take place over geologic space and time (Ford & Williams, 2007). Rammang-Rammang Karst Area is part of the Maros Karst cluster located in Salenrang Village and Bontolempangan Village, Bontoa District, Maros Regency, South Sulawesi. Astronomically, this area is located at 4°42'49"-5°06'42" S and 119°55'13" E. The total area of Maros-Pangkep Karst is 43,750 ha (Ahmad & Hamzah, 2016). This area is a tourist area and has a lot of natural resources potential and designated as Taman Nasional Geopark in Indonesia.

In this karst area there is a river that empties into the sea called the Sungai Pute. This river is one of the things that makes the Rammang-Rammang Maros Karst Area different from other karst areas in South Sulawesi. Tourist activities in the Rammang-Rammang Karst Area, including community-operated boat use, have contributed to erosion in the Sungai Pute. Ansar et al. (2014) identified rainfall, vegetation cover, organic material concentration, and human activities as key factors accelerating erosion, leading to increased turbidity, particularly near the dock area. According to the 2005 Decree of the Minister of Forestry, the sediment load in Sungai Pute is classified as high. This is evidenced by the

narrowing of the river channel near the dock. The resulting erosion elevates sedimentation rates, reduces the river's cross-sectional capacity, and alters wave propagation velocity. The decline in shear wave velocity subsequently affects the soil characteristics in the study area.

Shear wave velocity is one of the parameters to identify soil conditions and estimate specific ground motion hazards that can impact the bearing capacity of the soil around the area (Yusran et al., 2021). Soil layers with low density generally have low bearing capacity, making them prone to ground motion (Arisona et al., 2023). The study in the form of soil layer mapping using microtremor data aims to obtain an overview of soil layers that are potentially vulnerable to earthquake.

Microtremor are ambient ground vibrations occured due to natural causes or artificial disturbances such as traffic activities and industrial machineries (Anzehaee et al., 2025). Microtremor are applied to determine the dynamic characteristics such as the dominant period and amplification value of a sedimentary layer. The method used to process microseismic measurement data for open areas is the HVSR method (Nakamura, 2008). The HVSR method is used to determine the dominant frequency (f_0) and the peak value of HVSR (A) that represent the dynamic characteristics of sedimentary layers (Irjan & Bukhori, 2011). The dominant frequency and amplification value represent local geological conditions. Both parameters are influenced by the thickness of the sedimentary layer, so information about the thickness of the layer is very important when analysing the soil response (Mala et al., 2015). Shear wave velocity is related to soil sediment layer thickness and dominant frequency.

$$Vs = 4f_0H \tag{1}$$

where H is the sediment layer thickness (in m), Vs is the shear wave velocity (in m/s), and f_0 is the dominant frequency (in Hz) (Kanai, 1983).

Soft rocks or materials relatively have a smaller Vs value compared to hard rocks, because the shear wave velocity value is directly proportional to the density of the rock. The smaller density of the rock result the smaller shear wave velocity (Edison et al., 2022). Pudi et al. (2021) indicated that higher hilly areas are usually characterized by higher Vs, but weathering can be a very significant factor in Vs variations.

The Vs_{30} value is the average value of the shear wave velocity to a depth of 30 m, calculated based on the travel time of the wave from the surface to a depth of 30 m. The value of shear wave velocity to a depth of 30 m was first introduced by Brown et al. (2000). Shear wave velocity is recognized as an important parameter for evaluating soil dynamic properties. The value of Vs_{30} can be calculated by the following equation.

$$Vs_{30} = \frac{30}{\sum \frac{h_i}{Vs_i}} \tag{2}$$

where Vs_{30} is the shear wave velocity at a depth of 30 meters, h_i is the soil layer thickness, dan Vs_i is the shear wave velocity at the measurement point. Harder soil conditions produce higher shear wave velocities. This is because seismic waves can easily pass through denser soil, so the medium does not retain them and vice versa.

Table 1 NEHRP Soil Classification (Building Seismic Safety Council, 2004)

Site Class	Description	Vs_{30} (m/s)
S_A	Hard rock	> 1500
S_B	Rock with moderate weathering	760–1500
S_C	Very dense soil and Soft rock	360–760
S_D	Stiff soil	180–360
S_E	Soft soil	< 180

There are several criteria that categorise National Earthquake Hazard Reduction Provisions (NEHRP) site classes to determine local conditions based on Vs_{30} as in Table 1. In accordance with the Indonesian National Standard (SNI) 1726:2019 on earthquake-resistant design provisions for building and non-building structures, site classifications are provided as shown in Table 2.

Previous microseismic studies aimed at determining shear wave velocity have been conducted by several researchers. Mufardis et al. (2023) reported that, out of 16 scattered locations, Tracks 1, 3, and 5 in Banda Raya Subdistrict are classified as soft soil, with *Vs* values below 175 m/s. Tracks 2, 4, 6, 7, and 8 in Banda Raya Subdistrict, along with all tracks in Jaya Baru Subdistrict, are categorized as medium soil. Other research was conducted by Safitri et al. (2021) in the coastal area of Wangi-Wangi District, Wakatobi Regency, reporting shear wave velocities ranging from 319.74 to 2058.68 m/s. These values indicate the presence of very dense soil layers based on the SNI 1726 site classification.

Table 2 Soil Classification based SNI 1726 (Badan Standarisasi Nasional, 2019)

Class Site	Shear wave velocity Vs_{30} (m/s)
S_A (Hard rock)	≥ 1500
S_B (Rock)	$750 < Vs \leq 1500$
S_C (Very dense soil and soft rock)	$350 < Vs \leq 750$
S_D (Stiff soil)	$175 < Vs \leq 350$
S_E (Soft soil)	< 175

Arsyad et al. (2024) also utilized microtremor analysis to investigate dominant frequency, amplification, sediment thickness, and seismic vulnerability in the Rammang-Rammang Maros Karst Area. The distribution of 11 microtremor measurement points is presented in Figure 1. The results indicate that the highest sediment layer thicknesses occur near riverbanks, suggesting influence from both limestone weathering and river sedimentation. In contrast, thinner sediment layers in karst hills and residential areas indicate weathering predominantly due to limestone. Sediment thickness values range from 18.521 m to 88.029 m. The seismic vulnerability index *(Kg)* values range from 0.040 to 5.761. Since all values are below 6, the Rammang-Rammang Maros Karst Area is categorized as having low to moderate seismic vulnerability. The distribution of research points is uneven due to site conditions dominated by rivers and karst hills, which hinder data acquisition on irregular surfaces. Points 1–5 are clustered in the tourism area, located across the river and characterized by karst hills and rice fields. Points 6–11 form a semi-circular pattern covering the study area, which is mainly composed of residential areas and riverbanks.

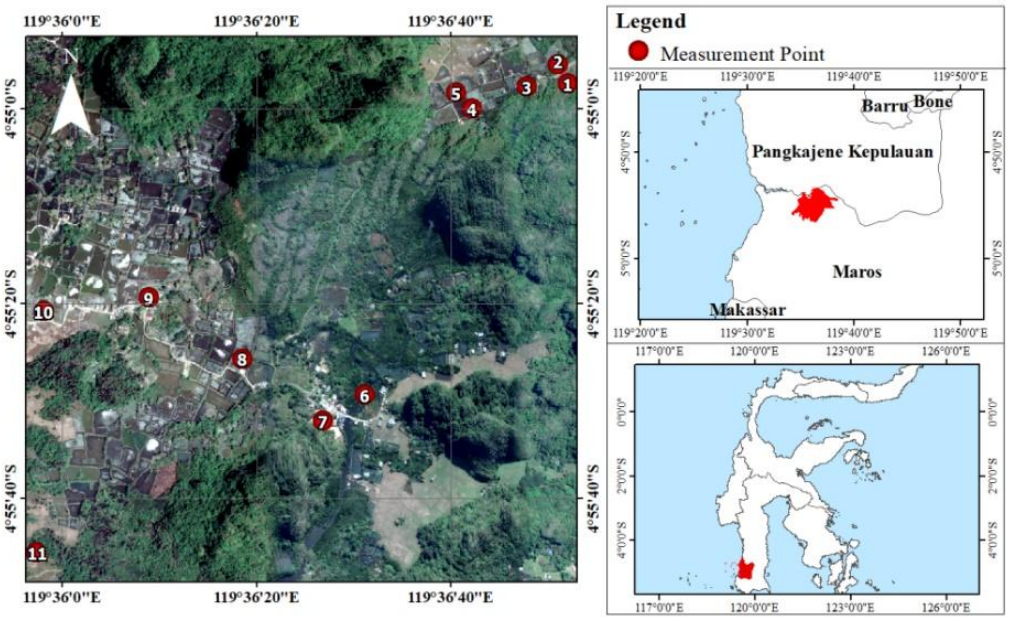

Figure 1 Location of Microtremor Measurement (Arsyad et al., 2024).

Shear wave velocity analysis was used to classify soil types at the study site. While previous microtremor studies have focused on seismically active regions, this research applies microtremor analysis in a karst environment to determine soil classification based on Vs_{30} values and to support land-

use planning in karst areas. The Vs_{30} values were derived through inversion of HVSR curves from raw microtremor data.

2. METHOD

Microtremor measurements were conducted in the Rammang-Rammang Karst Area, specifically in Salenrang and Bontolempangan Villages, Bontoa District, Maros Regency, South Sulawesi. Astronomically, the area is located between 4°54'51.61"–4°55'50.51" S and 119°35'30.38"–119°37'22.58" E. This study utilizes secondary data from Arsyad et al. (2024), consisting of raw microtremor recordings collected at the same locations, ensuring identical measurement point distribution (see Figure 1).

Both software and hardware instruments were employed. DataPro was used to convert microtremor recordings from hexadecimal to ASCII or MiniSEED (.MSD) format for further processing. Geopsy was used to generate HVSR curves, providing dominant frequency and amplification values. Dinver was applied to model the HVSR curves and derive shear wave velocity profiles with depth. The hardware consisted of a TDL-303S microtremor system, including a seismometer, digitizer, connection cable, GPS unit, and geological compass.

Measurement locations were selected in accordance with SESAME European Research Project (2004) guidelines. Measurements were conducted across approximately 2.62 km^2 at 11 points. As shown in Figure 1, the distribution is not uniform due to terrain limitations that prevented a loop layout. Therefore, the placement was adjusted based on SESAME (2004) standards, prioritizing flat ground, avoiding steep slopes, and maintaining distance from tall trees. Each recording lasted approximately 60 minutes, with an additional 5 minutes for points with higher ambient noise levels.

The microtremor data were processed using the HVSR analysis method. The recorded signals comprised three components: horizontal (East–West), horizontal (North–South), and vertical (Up–Down). Data in MiniSEED format were processed in Geopsy to obtain the horizontal-to-vertical (H/V) spectral ratio. Each signal component was analyzed using the Fast Fourier Transform (FFT) algorithm to convert the time-domain data into the frequency domain, producing a spectrum for each component (SESAME European Research Project, 2004).

$$F(w) = \int_{-\infty}^{\infty} f(t)^{-iwt} dt \tag{3}$$

where $F(w)$ is the Fourier transform of $f(t)$.

Subsequent processing in Geopsy involves filtering and windowing to remove high-noise signals, followed by the combination of signal components for HVSR analysis. The spectral ratio between the total horizontal and vertical components is then calculated using the following equation.

$$H/V = \frac{\sqrt{H_{EW}{}^2(f) + H_{NS}{}^2(f)}}{V_{UD}(f)} \tag{4}$$

where H/V is the spectrum ratio HVSR, $H_{EW}(f)$ is the horizontal component spectrum east-west, $H_{NS}(f)$ is the horizontal component spectrum north-south, and $V_{UD}(f)$ is the vertical component spectrum. The result of combining signals in HVSR analysis is an HVSR curve that present information about dominant frequency values and amplification.

The HVSR curves processed in Geopsy were further analyzed using Dinver software, employing the ellipticity curve method. This method, based on body-wave HVSR, enables the estimation of S-wave velocity at the microtremor measurement points. Ellipticity curve modeling allows the extraction of subsurface physical properties not accessible through the HVSR method alone. This method is then used to obtain surface shear wave velocity parameters in the form of a Vs ground profile at the measurement point. The ellipticity curve relies heavily on determining parameters that are close to experimental values by repetition. The accuracy of this process can be seen from the error (misfit). A smaller misfit value in the iteration process, result in a better shear wave velocity profile. Computational misfit can be calculated using the following equation.

$$misfit = \sqrt{\frac{1}{N}\sum_{i=1}^{N}\left(\frac{D_i - M_i}{\sigma_i}\right)^2} \quad (5)$$

where N is data point, Di is the inversion result data, dan M_i is the soil structure model.

The inversion of the HVSR curve will produce a ground profile of the soil shear wave velocity. The ground profile will show the final model from the measurement results and then the model with the lowest misfit value ($0 \leq misfit \leq 1$) will be selected.

3. RESULTS AND DISCUSSION

Microtremor data were processed using Geopsy to obtain dominant frequency and amplification. The HVSR curves in Figure 2 show different peak characteristics. Figure 2(a) shows a clear single peak, indicating a strong impedance contrast. Figure 2(b) shows multiple peaks, suggesting lateral subsurface variations.

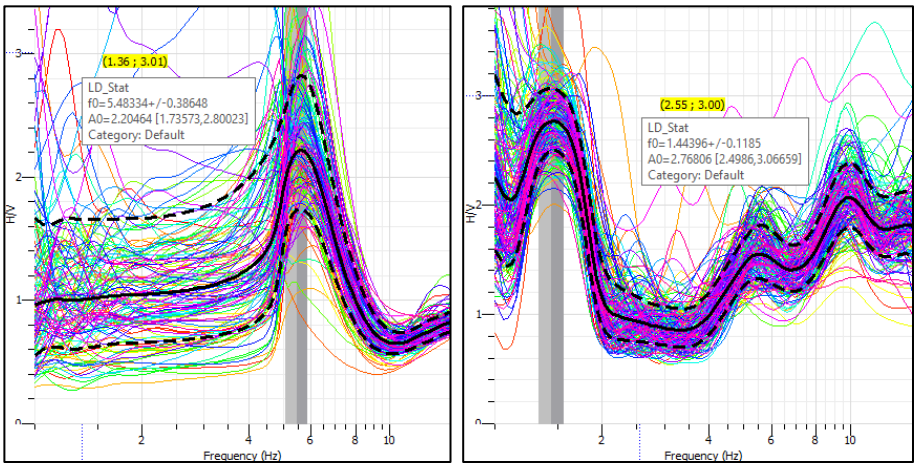

(a) (b)

Figure 2 HVSR curves (a) clear peak from P10 and (b) multiple peaks from P3 locations.

The dominant frequencies and amplification factors vary with site conditions, reflecting the subsurface lithology at each measurement point. These values are summarized in Table 3. Dominant frequencies range from 1.44 Hz to 6.21 Hz, and amplification values from 0.46 to 3.80. The lowest dominant frequency is recorded at point P3 (1.44 Hz), while the highest is at P2 (6.21 Hz). The lowest amplification is observed at P8 (0.46), and the highest at P6 (3.80).

Table 3 Microtremor data results at 4°54'57.3"-4°55'45.5" S and 119°35'58.1"-119°36'52.0" E

Point	Coordinate		f_0 (Hz)	A_0
	Latitude (S)	Longitude (E)		
P1	4°54'57.3"	119°36'52.0"	5.48433	1.26007
P2	4°54'55.3"	119°36'51.0"	6.20859	2.47336
P3	4°54'57.6"	119°36'47.8"	1.44396	2.76806
P4	4°54'59.9"	119°36'42.2"	3.79734	1.78686
P5	4°54'58.2"	119°36'40.5"	2.08152	1.01565
P6	4°55'29.3"	119°36'31.1"	5.27442	3.79584
P7	4°55'32.0"	119°36'26.8"	5.77950	0.80887
P8	4°55'25.6"	119°36'18.5"	5.49075	0.45676
P9	4°55'19.3"	119°36'08.9"	4.60779	1.95681
P10	4°55'20.7"	119°35'58.1"	5.48334	2.20464
P11	4°55'45.5"	119°35'57.3"	4.13763	1.55908

The distribution of dominant frequencies in the Rammang-Rammang Maros Karst Area, based on HVSR analysis, is shown in Figure 3. High dominant frequencies (red and yellow) are concentrated

in karst hills and residential areas, while low frequencies (blue and green) are observed near rivers and rice fields.

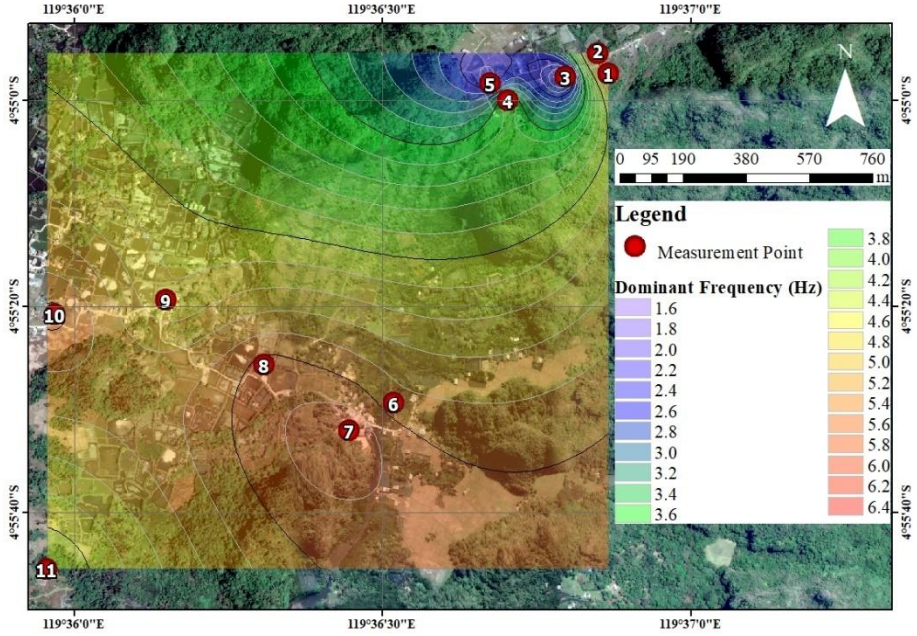

Figure 3 Map of the Distribution of Dominant Frequency of the Rammang-Rammang Maros Karst Area.

The distribution of amplification values in the Rammang-Rammang Maros Karst Area based on HVSR analysis, is shown in Figure 4. High amplification values (shown in red) are concentrated around the river, while low values (blue and green) are observed in karst hilly areas, residential zones, and near rice fields.

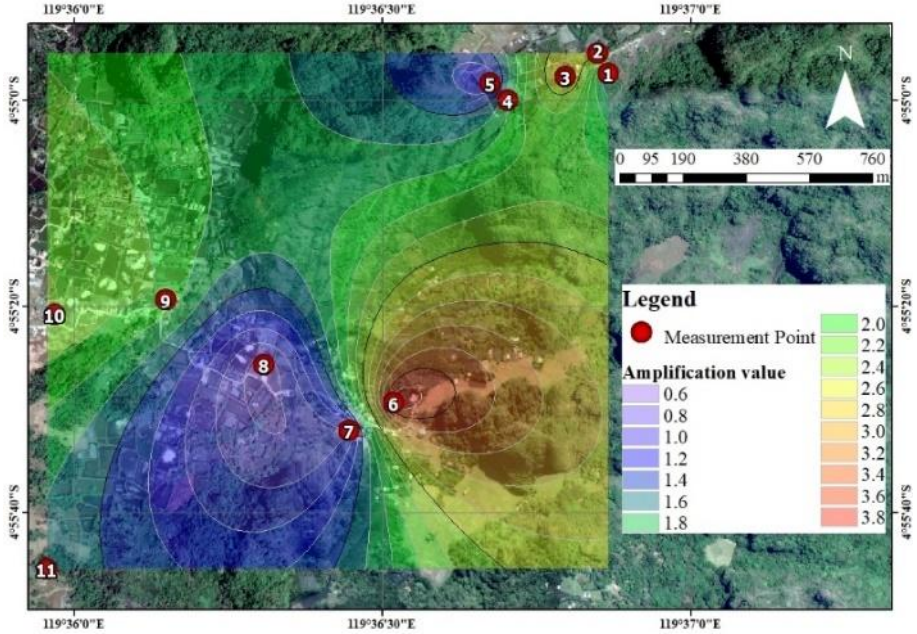

Figure 4 Map of the Distribution of Amplification Values of the Rammang-Rammang Maros Karst Area

The HVSR curves were inverted using Dinver to obtain shear wave velocity profiles for each measurement point, which are used to classify soil types at the study site. The resulting ground profiles from the inversion at selected points are displayed in Figure 5. It illustrates the ground profile inversion

results, where the brightest red line represents the model with the lowest misfit value, while the other lines represent the range of plotted models. The number of models plotted for each measurement point varies depending on the characteristics of the HVSR curves derived from previous data processing. From the HVSR inversion results, shear wave velocity at a depth of 30 meters is calculated using Equation (2). The resulting shear wave velocity values for each point are presented in Table 4.

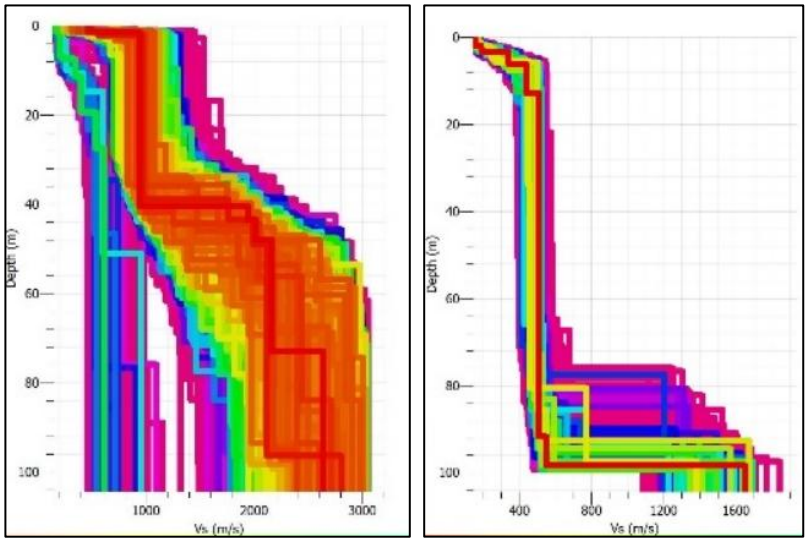

(a) (b)

Figure 5 (a) Ground profile of P10 and (b) Ground profile of P3 locations.

The shear wave velocity values obtained in this study are presented in Table 4, ranging from 249.28 to 1384.03 m/s. Point P8 recorded the lowest value (249.28 m/s), while P1 recorded the highest (1384.03 m/s). Low to medium velocities (200–750 m/s), typically associated with clay, alluvial, and silt deposits, were observed near rivers, residential areas, and rice fields. High velocities (>750 m/s), corresponding to limestone, were found in the karst hilly areas.

Table 4 The HVSR inversion results at coordinates 4°54'57.3"-4°55'45.5" S and 119°35'58.1"-119°36'52.0" E.

Point	Coordinate		Vs_{30} (m/s)	Lithology
	Latitude (S)	Longitude (E)		
P1	4°54'57.3"	119°36'52.0"	1384.03	Limestone
P2	4°54'55.3"	119°36'51.0"	692.23	Silt
P3	4°54'57.6"	119°36'47.8"	505.12	Alluvial
P4	4°54'59.9"	119°36'42.2"	813.12	Limestone
P5	4°54'58.2"	119°36'40.5"	476.83	Alluvial
P6	4°55'29.3"	119°36'31.1"	799.21	Limestone
P7	4°55'32.0"	119°36'26.8"	334.16	Clay
P8	4°55'25.6"	119°36'18.5"	249.28	Clay
P9	4°55'19.3"	119°36'08.9"	536.66	Silt
P10	4°55'20.7"	119°35'58.1"	840.19	Limestone
P11	4°55'45.5"	119°35'57.3"	530.54	Silt

The distribution of shear wave velocity values to a depth of 30 meters in the Rammang-Rammang Maros Karst Area, based on HVSR curve inversion, is shown in Figure 6. High shear wave velocities (indicated in red) are concentrated in the karst hilly areas, while low velocities (shown in blue and green) are observed near rivers, residential areas, and rice fields.

Rock classification is based on subsurface data up to 30 meters depth, as only layers within this range influence seismic wave amplification (Wangsadinata, 2006). Therefore, the Vs_{30} value is used to classify soil and rock types according to their response to local seismic effects. The classification based

on NEHRP standards is presented in Table 5. Three site classes are identified in the study area: four points classified as rock, five points as soft rock, and two points as stiff soil.

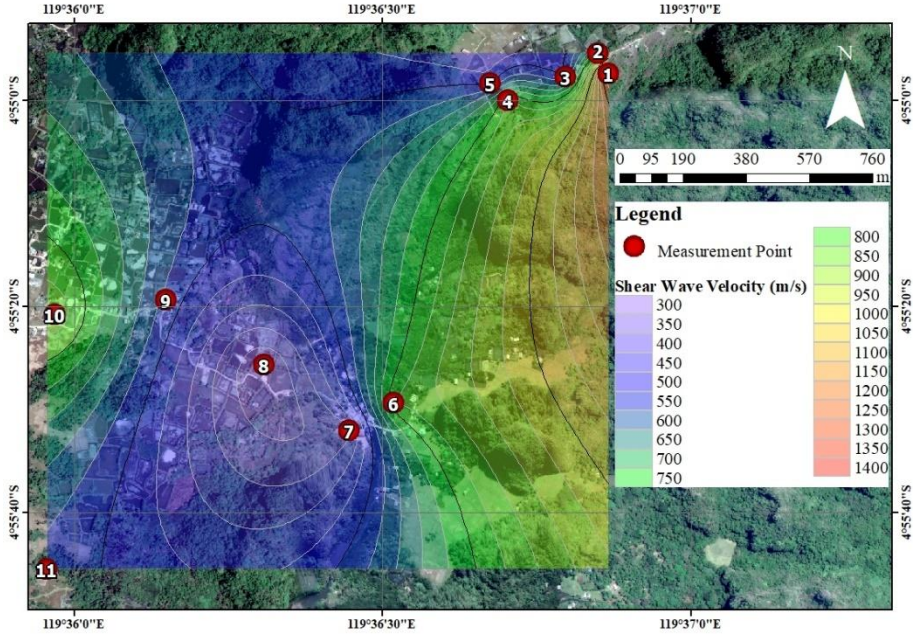

Figure 6 Map of the Distribution of Shear Wave Velocity Values of the Rammang-Rammang Maros Karst Area.

Table 5 NEHRP soil classification based on shear wave velocity.

Site Class	Vs_{30} (m/s)	Point	Description
S_B	760–1500	P1, P4, P6, P10	Rock with moderate weathering
S_C	360–760	P2, P3, P5, P9, P11	Very dense soil and soft rock
S_D	180–360	P7, P8	Stiff soil

According to the SNI classification, the corresponding soil and rock types based on shear wave velocity are presented in Table 6. Three site classes are identified within the study area: four points are classified as rock *(S_B)*, five points as soft rock *(S_C)*, and two points as stiff soil *(S_D)*. Site Class *(S_B)*, representing rock, is associated with limestone; *(S_B)*, representing soft rock, with silt and alluvial deposits; and *(S_D)*, representing stiff soil, with clay.

Table 6 Classification of soil types by SNI 1726:2019 based on shear wave velocity.

Site Class	Vs_{30} (m/s)	Point	Rock/Soil type
S_B (Rock)	$750 < Vs \leq 1500$	P1, P4, P6, P10	Limestone
S_C (Very dense soil and soft rock)	$350 < Vs \leq 750$	P2, P3, P5, P9, P11	Silt and alluvial
S_D (Stiff soil)	$175 < Vs \leq 350$	P7, P8	Clay

Figures 3 and 6 indicate that lower shear wave velocities and dominant frequencies are generally observed near residential areas, rivers, and rice fields, whereas higher values are found in karst hilly regions. The low velocities in the former are likely due to unconsolidated materials resulting from limestone weathering and river sedimentation. In contrast, the higher velocities in the karst hills are primarily associated with more compact, weathered limestone formations.

Permana et al. (2025) conducted research in Gorontalo using microtremor data for soil classification, revealing a broader distribution of soft soils compared to previous geomorphology-based studies. Approximately 36% of Gorontalo City is classified as soft soil, with the lowest Vs_{30} value of 131 m/s recorded near Danau Limboto, extending to the Sungai Bone mouth in the city's southern area. Similar findings were observed in the Rammang-Rammang Maros Karst Area, where soft soils were also identified near water bodies, particularly rivers, with the lowest Vs_{30} value of 249.28 m/s, still higher than the value reported in the Gorontalo study. Meanwhile, Yusran et al. (2021) reported Vs_{30} values

ranging from 200 to 250 m/s in Banda Aceh City, attributed to soft-to-hard rock transitional formations. These conditions result in a relatively high seismic vulnerability index and potential amplification of earthquake waves.

Shear wave velocity is influenced by two main variables: dominant frequency and sediment thickness. The study results indicate that high dominant frequencies do not consistently correspond to high shear wave velocities, due to variations in sediment thickness across the study area. While higher dominant frequencies generally suggest higher shear wave velocities, the relationship is modulated by sediment thickness. According to Fadhilah et al. (2023), regions with hard rock and thin sediment typically exhibit high natural frequencies, whereas areas with soft rock and thick sediment tend to show low natural frequencies.

A graph was plotted by Rahman et al. (2023) using a shear wave velocity value of 200 m/s to represent a very hard soil structure and 10 m/s to represent a soil structure with low permeability (sand). It is found that at low shear wave velocity, soil is in uncompacted state, resulting in reduced shear strength. Therefore, soil erosion occurs easily in the area. Based on that research, it was found that the potential risk of an earthquake occurring at the research location is low because the shear wave velocity value obtained is more than 200 m/s. Edison et al. (2021) conducted a research on the Cilacap coast and classified the area into soft, medium, and hard soil types based on Vs_{30} values. In Tritih Kulon as the research area, higher levels of earthquake damage were observed, associated with its soil classification and low Vs_{30} values ranging from 6.68 to 461.24 m/s. These values differ significantly from those obtained in the Rammang-Rammang Maros Karst Area, indicating lower seismic vulnerability at this research area.

The lowest shear wave velocity was recorded at point P8, with a value of 249.28 m/s. This is attributed to its location near rice fields, where the soil is relatively soft compared to other sites. Low Vs_{30} values indicate slower wave propagation in soft soils, causing seismic energy to remain longer at the surface and increasing potential damage during an earthquake. Areas with low Vs_{30} are thus considered highly vulnerable, indicating that the sediment strength in these regions is very weak, so development needs to be adjusted to the characteristics site effect of this area.

4. CONCLUSION

This study demonstrates that the variation in shear wave velocity (Vs) reflects the diverse geological conditions of the Rammang-Rammang Karst Area. These variations are primarily influenced by limestone weathering and river sedimentation. Based on Vs_{30} values derived from HVSR curve inversion at 11 measurement points, three site classes were identified: four points classified as rock (Vs_{30} 760–1500 m/s) in the karst hills, five points as soft rock (Vs_{30} 360–760 m/s) near residential areas and rivers, and two points as stiff soil (Vs_{30} 180–360 m/s) near rice fields. These findings suggest that areas with low Vs_{30} values—particularly those near rivers and rice fields—have higher sedimentation risks and should be developed with caution. In contrast, zones with higher $Vs30$ values are more geologically stable and thus more suitable for development, provided that karst features are preserved. The amplification values, all below 6, along with Vs values exceeding 200 m/s, indicate a relatively low seismic risk in the study area. This research highlights the effectiveness of HVSR curve inversion using dominant frequency and amplification to assess subsurface conditions. For future studies, expanding the measurement network is recommended to improve the resolution and accuracy of microzonation maps.

ACKNOWLEDGEMENT

This research was supported by Badan Meteorologi Klimatologi dan Geofisika (BMKG) through the provision of seismometers for microtremor data acquisition

REFERENCE

Ahmad, A., & Hamzah, A. S. (2016). *Database Karst Sulawesi Selatan*. Makassar: Badan Lingkungan Hidup Provinsi Sulawesi Selatan.

Ansar, N. A., Arsyad, M., & Sulistiawaty. (2014). Studi Analisis Sedimentasi di Sungai Pute Rammang-Rammang Kawasan Karst Maros. Jurnal Sains dan Pendidikan Fisika, 10(3), 301- 307. https://doi.org/10.35580/jspf.v10i3.968

Anzehaee, M. M., Adib, A., & Heydarzadeh, K. (2015). Improvement of Microtremor Data Filtering and Processing Methods Used in Determining the Fundamental Frequency of Urban Areas. *Pure and Applied Geophysics*, 172, 2859-2869. https://doi.org/10.1007/s00024-015-1097-7

Arisona, Manginsih, S. L., Praja, N. K., Hazria, & Azhar. (2023). Pemetaan Lapisan Tanah Menggunakan Data Mikrotremor HVSR dan Dampaknya Terhadap Daya Dukung Tanah di Kawasan Kota Kendari. *Jurnal Geologi dan Sumberdaya Mineral*, 24(1), 51-58. https://doi.org/10.33332/jgsm.geologi.v24i1.724

Arsyad, M., Hasaniyah, S., & Susanto, A. (2024). Investigation of Sediment Thickness in The Rammang-Rammang Maros Karst Area Using Microtremor Method. *Journal of Physics: Conference Series*, 2734, 1-10. https://doi.org/10.1088/1742-6596/2734/1/012020

Badan Standarisasi Nasional. (2019). *Standar Nasional Indonesia (SNI) 1726-2019: Tata Cara Perencanaan Ketahanan Gempa Untuk Struktur Bangunan Gedung Dan Nongedung.* Jakarta: Badan Standarisasi Nasional.

Brown. L., Diehl, J. G., & Nigbor, R. L. (2000). *A Simplified Procedure To Measure Average Shear-Wave Velocity to a Depth of 30 Meters (Vs_{30}).* Proceedings of The 12th World Conference On Earthquake Engineering (pp. 1–8). Auckland, New Zealand.

Building Seismic Safety Council (2004). *NEHRP Recommended Provisions for Seismic Regulations for New Builidings and Other Structures (FEMA 450)* (2003 ed.). Washington. D.C: National Institute of Building Science.

Edison, R., Prakoso, W. A., & Rohadi, S. (2022). Pemetaan Vs_{30} Dengan Menggunakan Korelasi Zhao Di Pesisir Cilacap. *Jurnal Geosaintek*, 8(1), 181-190. http://dx.doi.org/10.12962%2Fj25023659.v8i1.12601

Fadhilah, F.H., Yudistira, T., & Tohari, A. (2023). Soil Dynamic Response Mapping and Vulnerability Analysis of Earthquake Hazard in Banda Aceh Using HVSR Method. *IOP Conference Series: Earth and Environmental Science,* 1288, 1-8. https://doi.org/10.1088/1755-1315/1288/1/012021

Ford, D., & Williams, P. (2007). *Karst Hydrogeology and Geomorphology*. Sussex: John Wiley & Sons.

Irjan & Bukhori, A. (2011). Pemetaan Wilayah Rawan Bencana Berdasarkan Data Mikroseismik menggunakan TDS (Time Digital Seismograph) Tipe 303 S. *Jurnal Neutrino*, 3(2), 153-162. http://dx.doi.org/10.12962%2Fj25023659.v8i1.12601

Kanai, K. (1983). *Engineering Seismology.* Tokyo: University of Tokyo Press.

Mala, H. U., Adi, S., & Sunaryo. (2015). Kajian Mikrotremor dan Geolistrik Resistivitas di Sekitar Jalan Arteri Primer Trans Timor Untuk Mitigasi Bencana. *Natural B*, 3 (1), 24-34. https://doi.org/10.21776/ub.natural-b.2015.003.01.4

Mufardis, A., Khaizal, & Irwandi. (2023). Pemetaan Vs30 dan Analisis Potensi Likuifaksi Berdasarkan Vs Menggunakan Metode MASW di Kecamatan Banda Raya dan Jaya Baru Kota Banda Aceh. *Journal of The Civil Engineering Student*, (5)1, 162-168. https://doi.org/10.24815/journalces.v5i2.20992

Nakamura, Y. (2008). *On The H/V Spectrum*. Proceedings of The 14th World Conference on Earthquake Engineering. Beijing, China.

Permana, D., Widiyantoro, S., Persada, Y. D., & Habibah, N. (2025). Soil Classification Mapping by Vs_{30} MASW Measurements in Gorontalo City. *IOP Conference Series: Earth and Environmental Science,* 1458, 1-10. https://doi.org/10.1088/1755-1315/1458/1/012031

Pudi, R., Roy, P., Martha. T. R., & Kumar, K. V. (2021). Estimation of Earthquake Local Site Effects Using Microtremor Observations For The Garhwal–Kumaun Himalaya. India. *Near Surface Geophysics*, 19(1), 73-93. https://doi.org/10.1002/nsg.12128

Rahman, N. A., Rehman, M. A., Zahari, N. A., Taib, A. M., Mohtar, W. H. M. W., Ramli, A. B., Ibrahim, A., Hasbollah, D. Z. A., Mitu, S. M., & Nurdin, M. F. (2023). The Potential of Shear Wave Velocity as an Erosion Risk Index. *Physics and Chemistry of the Earth, Parts A/B/C*, 129. http://dx.doi.org/10.1016/j.pce.2022.103302

Safitri, A., Hamimu, L., & Manan, A. (2021). Inversi HVSR Data Mikrotremor untuk Penentuan Kecepatan Gelombang Shear (S) di Daratan Pesisir Kecamatan Wangi-Wangi Kabupaten Wakatobi. *Jurnal Rekayasa Geofisika Indonesia*, 3(1), 1-8. https://doi.org/10.56099/jrgi.v3i01.16647

SESAME European Research Project. (2004). *Guidelines for The Implementation of The H/V Spectral Ratio Technique on Ambient Vibrations. Measurement. Processing. and Interpretation*. European Commision: Research General Directorate.

Wangsadinata, W. (2006). *Perencanaan Bangunan Tahan Gempa Berdasarkan SNI 1726-2002. Shortcourse HAKI 2006*. Jakarta.

Yusran , Simanjuntak, A. V. H., Umar, M., & Rahmati. (2021). Analisis Kerentanan Seismik dan Model Vs_{30} Berdasarkan Survei Mikrotremor HVSR dan SPAC (Studi Kasus: Kota Banda Aceh). *Jurnal Lingkungan dan Bencana Geologi*, 12(2), 125-136. http://dx.doi.org/10.34126/jlbg.v12i2.324